Electronic Supplementary Material (ESI) for Energy & Environmental Science

Electronic Supporting Information

$K_7[Co^{III}Co^{II}(H_2O)W_{11}O_{39}]$: A Molecular Mixed-valence Keggin Polyoxometalate Catalyst of High Stability and Efficiency for Visible Light-driven Water Oxidation

Fangyuan Song [a], Yong Ding [a]*, Baochun Ma [a]*, Changming Wang [a], Qiang Wang [a], Xiaoqiang Du [a], Shao Fu [a], Jie Song[b]*

[a] State Key Laboratory of Applied Organic Chemistry, Key Laboratory of Nonferrous Metals Chemistry and Resources Utilization of Gansu Province and College of Chemistry and Chemical Engineering, Lanzhou University, Lanzhou 730000, China.
[b] Department of Biomedical Engineering, Emory University and Georgia Institute of Technology, Atlanta, Georgia 30322, USA

* To whom correspondence should be addressed.
E-mail addresses: dingyong1@lzu.edu.cn, mabaochun@lzu.edu.cn, jsong7@emory.edu

Experimentals and calculation

UV-vis tracking of Control Experiments (in absent of catalyst 1)

An 18 mL of pH 9.0, 80 mM borate buffer containing 1 mM of photosensitizer and 5 mM of $Na_2S_2O_8$ without catalyst was irradiated for 4 min. Then the UV-vis spectra of the solution were measured. Using 18 mL of pure water replaced above borate buffer, then the same operation was executed. The solution color turned to green after 30 s of irradiation.

Bond valence sum (BVS) calculation

$$\text{The valence sum} = \sum \exp[(d_0 - d)/B]$$

d_0 =1.692 for Co, B = 0.37, Four values of d(Co-O) are the same (1.82).

$$\text{The valence sum} = \sum \exp[(1.692 - 1.82)/0.37]$$
$$= 4 \times \exp[(1.692 - 1.82)/0.37] = 2.8 \approx 3$$

Quantum yield calculation

Initial O_2 formation rate = 0.069 μmol.s^{-1}

Irradiation radius =1 cm =0.01 m

Photon flux = π× (0.01m)^2 × 1650 μmol.m^{-2}.s^{-1}=0.518 μmol.s^{-1}

$$\Phi_{QY(initial)} = 2 \times \frac{\text{initial } O_2 \text{ formation rate}}{\text{photon flux}} \times 100\%$$
$$= \frac{2 \times 0.069 \mu mol \bullet s^{-1}}{0.518 \mu mol \bullet s^{-1}} \times 100\%$$
$$= 27\%$$

Table S1. Crystallographic data and structure refinement for $K_7[Co^{III}Co^{II}(H_2O)W_{11}O_{39}]$ (**1**)

Empirical formula	$Co_2\ K_7\ O_{49}\ W_{11}$
Formula weight	3197.91 g mol^{-1}
Crystal system	Cubic
Space group	Fm-3m
Unit cell	a = 21.2598(4) Å *b* = 21.2598(4) Å *c* = 21.2598(4) Å α= 90° β= 90° γ= 90°
Volume	9609.0(3) $Å^3$
Z	8
Density (calcd)	4.421 g cm^{-3}
Temperature	100(2)K
Wavelength	0.71073 Å
Absorption coefficient	27.604 mm^{-1}
Reflections collected	2248
Independent reflections	504 [R(int) = 0.0321]
GOF	1.092
Final R indices [$I>2\sigma(I)$]	$R_1{}^a$ = 0.0284, $wR_2{}^b$ = 0.0975
R indices (all data)	$R_1{}^a$= 0.0330, $wR_2{}^b$ = 0.1008

$^aR_1 = \Sigma||F_0| - |F_c|| / \Sigma|F_0|$; $wR_2 = \Sigma[w(F_0^2 - F_c^2)^2]/\Sigma[w(F_0^2)^2]^{1/2}$

Table S2 Physical property of compound **1-4**

Catalyst	Color	Shape
$K_7[Co^{III}Co^{II}(H_2O)W_{11}O_{39}]$ (**1**)	dark brown	cube
$K_6[Co^{II}W_{12}O_{40}]$ (**2**)	bluish green	prism
$K_5[Co^{III}W_{12}O_{40}]$ (**3**)	golden yellow	prism
$K_8[Co^{II}Co^{II}(H_2O)W_{11}O_{39}]$ (**4**)	emerald green	cube

Table S3. TON and $TOF_{initial}$ of water oxidation catalyzed by different catalysts

Catalyst	Representative reaction conditions	TON	TOF	Ref.
1	LED lamp ($\lambda \geq 420$ nm), 1.0 mM $[Ru(bpy)_3]Cl_2$, 5.0 mM $Na_2S_2O_8$, 80 mM sodium borate buffer (pH 9.0)	361 (Based on 1 μM **1**) [a]	0.5 s^{-1} (Based on 5 μM **1**) [a]	This work
$Na_{10}[Co_4(H_2O)_2(\alpha\text{-}PW_9O_{34})_2]$	Xe lamp (420–470 nm), 5 μM catalyst, 1.0 mM $[Ru(bpy)_3]Cl_2$, 5.0 mM $Na_2S_2O_8$, 80 mM sodium borate buffer (pH 8.0)	224	No data	1
$K_{10.2}Na_{0.8}[\{Co_4(\mu\text{-}OH)(H_2O)_3\}(Si_2W_{19}O_{70})]$	Xe lamp (420–520 nm), 10 μM catalyst, 1.0 mM $[Ru(bpy)_3]Cl_2$, 5 mM $Na_2S_2O_8$, 25 mM sodium borate buffer (pH 9.0)	80	0.1 s^{-1}	2
$(NH_4)_3[CoMo_6O_{24}H_6]$	300 W Xe lamp (400–800 nm), 0.4 mM $[Ru(bpy)_3](NO_3)_2$, 3 mM $Na_2S_2O_8$, 0.1 M borate buffer solution (pH 8.0)	107 (Based on 3.6 μM catalyst)	0.11 s^{-1} (Based on 20 μM catalyst)	3
$(NH_4)_6[Co_2Mo_{10}O_{38}H_4]$	300 W Xe lamp (400–800 nm), 0.4 mM $[Ru(bpy)_3](NO_3)_2$, 3 mM $Na_2S_2O_8$, 0.1 M borate buffer solution (pH 8.0)	154 (Based on 1.9 μM catalyst)	0.16 s^{-1} (Based on 10 μM catalyst)	3
$K_{11}Na_1[Co_4(H_2O)_2(SiW_9O_{34})_2]$	LED lamp (470 nm), 1 mM $[Ru(bpy)_3]Cl_2$, 5 mM $Na_2S_2O_8$, 20 mM Na_2SiF_6 buffer (pH 5.8)	24 (Based on 20 μM catalyst)	0.4 s^{-1} (Based on 42 μM catalyst)	4
Trans-$[Co^{II}(qpy)(OH_2)_2](ClO_4)_2$	500 W mercury arc lamp (457 nm), 0.2 μM catalyst, 128 μM $[Ru(bpy)_3]Cl_2$, 5 mM $Na_2S_2O_8$, 15 mM borate buffer solution (pH 8.0)	355 (Reaction time = 1.5 h)	No data	5
$[Co^{II}(Me_6tren)(OH_2)](ClO_4)_2$ (Decomposed to $Co(OH)_x$)	500 W Xe lamp ($\lambda > 420$ nm), 5.0 μM catalyst, 0.5 mM $[Ru(bpy)_3](ClO_4)_2$, 10 mM $Na_2S_2O_8$, 100 mM borate buffer solution (pH 9.0)	420	No data	6
$[Co^{III}(Cp^*)(bpy)(OH_2)](PF_6)_2$ (Decomposed to $Co(OH)_x$)	500 W Xe lamp ($\lambda > 420$ nm), 5.0 μM catalyst, 0.5 mM $[Ru(bpy)_3](ClO_4)_2$, 10 mM $Na_2S_2O_8$, 100 mM borate buffer solution (pH 9.0)	320	No data	6
$Co^{III}_4O_4(OAc)_4(py)_4$	250W high power Arc lamp (450 nm), 41.5 μM catalyst, 0.5 mM $[Ru(bpy)_3]Cl_2$, 10.5 mM $Na_2S_2O_8$, HCO_3^- buffer (pH 7.0)	40	0.02 s^{-1}	7
TiO_2	LED lamp ($\lambda \geq 420$ nm), 27 mg	0 [b]	0 [b]	This

	TiO_2, 1.0 mM $[Ru(bpy)_3]Cl_2$, 5.0 mM $Na_2S_2O_8$, 80 mM sodium borate buffer (pH 9.0)			work
$Fe(ClO_4)_3$ (Formed Fe_2O_3)	200 W Xe lamp, λ > 420 nm, 1.0 μM catalyst, 0.2 mM $[Ru(bpy)_3]Cl_2$, 2 mM $Na_2S_2O_8$, 15 mM borate buffer (pH 8.5)	436	No data	8
$Fe(mcp)Cl_2$ (Decomposed to Fe_2O_3)	200 W Xe lamp, λ > 420 nm, 1.0 μM catalyst, 0.2 mM $[Ru(bpy)_3]Cl_2$, 2 mM $Na_2S_2O_8$, 15 mM borate buffer (pH 8.5)	194	No data	8
$[Fe(bpy)_2Cl_2]Cl$ (Decomposed to Fe_2O_3)	200 W Xe lamp, λ > 420 nm, 1.0 μM catalyst, 0.2 mM $[Ru(bpy)_3]Cl_2$, 2 mM $Na_2S_2O_8$, 15 mM borate buffer (pH 8.5)	157	No data	8
$[Fe(tpy)_2]Cl_2$ (Decomposed to Fe_2O_3)	200 W Xe lamp, λ > 420 nm, 1.0 μM catalyst, 0.2 mM $[Ru(bpy)_3]Cl_2$, 2 mM $Na_2S_2O_8$, 15 mM borate buffer (pH 8.5)	376	No data	8
$[Fe(cyclen)Cl_2]Cl$ (Decomposed to Fe_2O_3)	200 W Xe lamp, λ > 420 nm, 1.0 μM catalyst, 0.2 mM $[Ru(bpy)_3]Cl_2$, 2 mM $Na_2S_2O_8$, 15 mM borate buffer (pH 8.5)	412	No data	8
$Fe(tmc)Br_2$ (Decomposed to Fe_2O_3)	200 W Xe lamp, λ > 420 nm, 1.0 μM catalyst, 0.2 mM $[Ru(bpy)_3]Cl_2$, 2 mM $Na_2S_2O_8$, 15 mM borate buffer (pH 8.5)	364	No data	8

[a] $TOF_{initial}$ = $TON_{initial}$/60 s, $TON_{initial}$= Molar of oxygen produced in 1 minute/Molar of **1**.

[b] Subtracting of the blank.

Table S4. Photocatalytic water oxidation catalyzed by **1**.[a]

1 (μM)	buffer	Initial pH	Capacity (mM)	$[Ru(bpy)_3]^{2+}$ (mM)	$Na_2S_2O_8$ (mM)	Yield (%)[b]	O_2 (μmol)[c]	TON[d]
15	borate	9.0	80	1	5	30	13.7	51
15	phosphate	9.0	80	1	5	4.5	2.0	7.5
15	carbonate	9.0	80	1	5	5.5	2.5	9.1
15	borate	8.0	80	1	5	16.0	7.2	27
15	borate	10.0	80	1	5	21.6	9.7	36
15	borate	9.0	60	1	5	31.1	14.0	52
15	borate	9.0	40	1	5	32.0	14.4	53
15	borate	9.0	20	1	5	26.4	11.9	44
15	borate	9.0	90	1	5	25.8	11.6	43
15	borate	9.0	80	0.7	5	26.2	11.8	44
15	borate	9.0	80	0.4	5	24.4	11	41
15	borate	9.0	80	1.5	5	19.9	8.9	33
15	borate	9.0	80	0	5	0	0	0
15	borate	9.0	80	1	4	31.1	11.2	41
15	borate	9.0	80	1	2	31.8	5.7	21
15	borate	9.0	80	1	7	19.2	12.1	45
15	borate	9.0	80	1	0	0	0	0
10	borate	9.0	80	1	5	28.2	12.7	71
5	borate	9.0	80	1	5	20.2	9.1	101
1	borate	9.0	80	1	5	14.4	6.5	361
20	borate	9.0	80	1	5	26.2	11.8	33
0	borate	9.0	80	1	5	1.4	0.6	

[a] O_2 evolution in the presence of additional components listed in this table, and other reaction conditions were the same as **Table 1**(in maintext).

[b] O_2 yield = 2 × mole of O_2/mole of $Na_2S_2O_8$

[c] The amount of O_2 evolved from 18 mL reaction solution after 10 min of irradiation.

[d] Based on the amount of O_2 produced after 10 min irradiation.

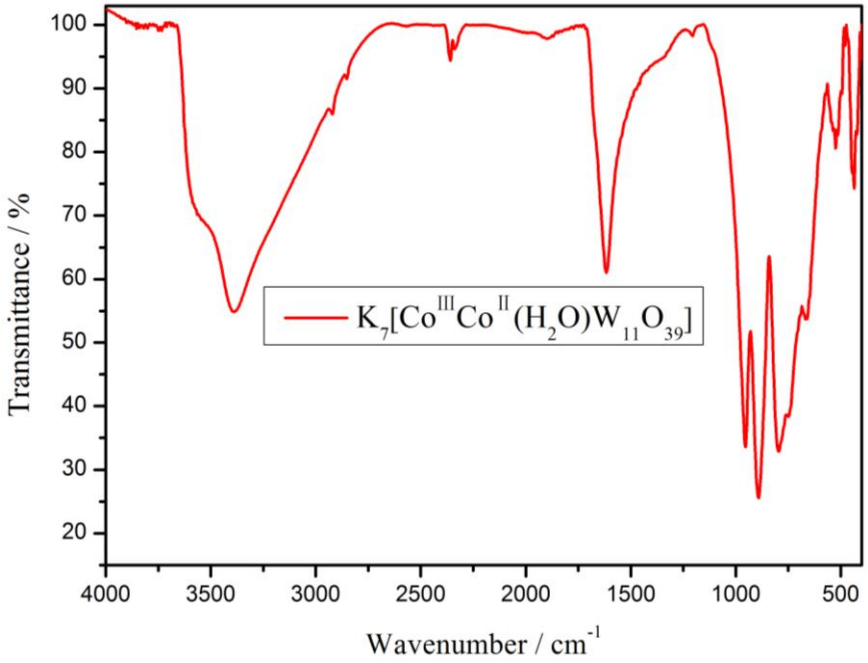

Fig. S1 FT-IR spectrum of **1**.

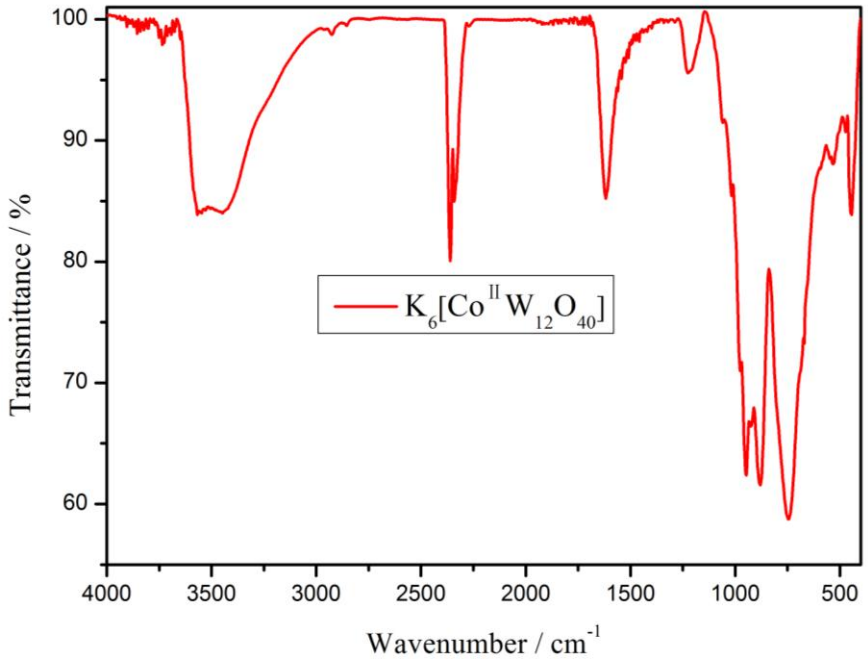

Fig. S2 FT-IR spectrum of **2**.

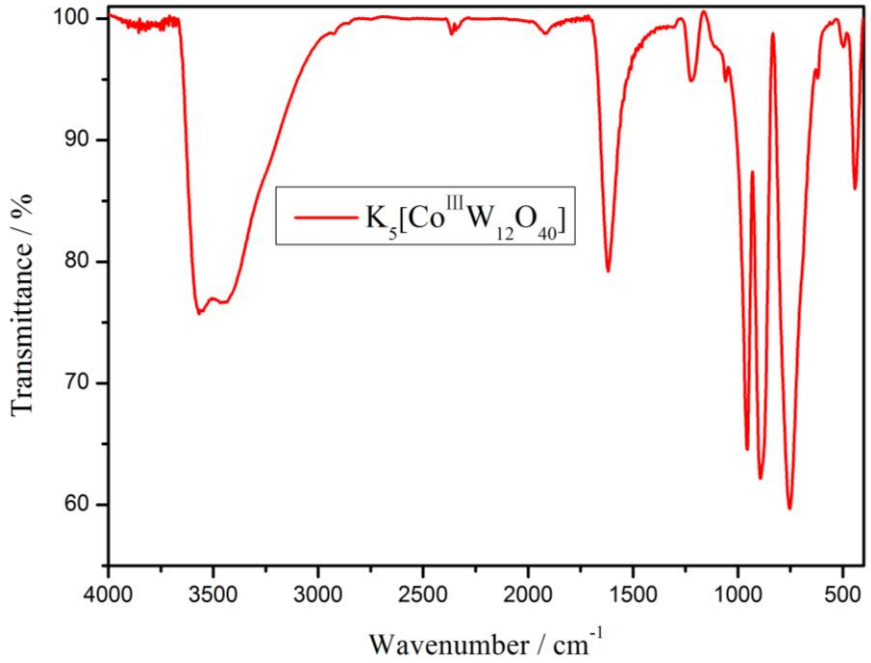

Fig. S3 FT-IR spectrum of **3**.

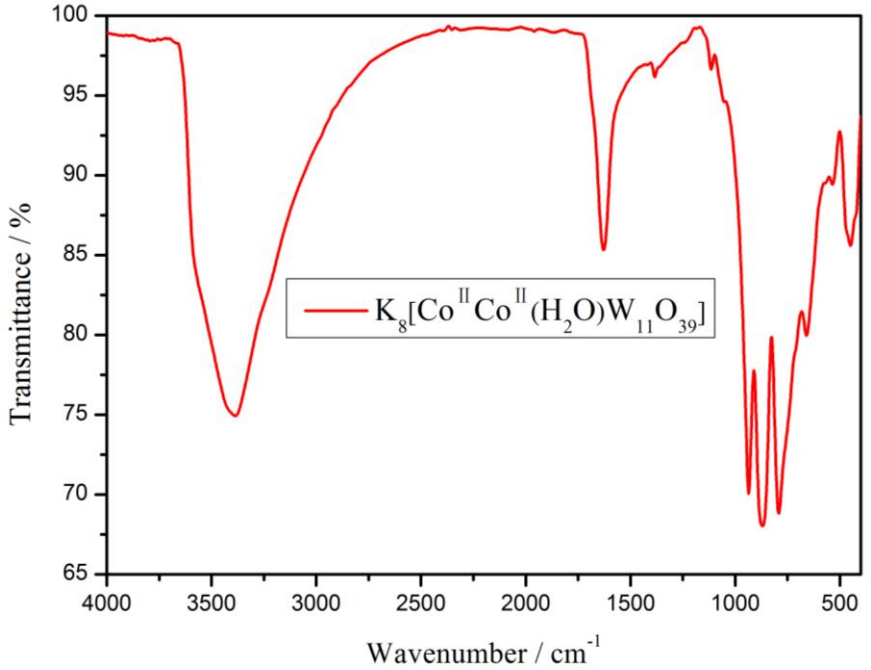

Fig. S4 FT-IR spectrum of **4**.

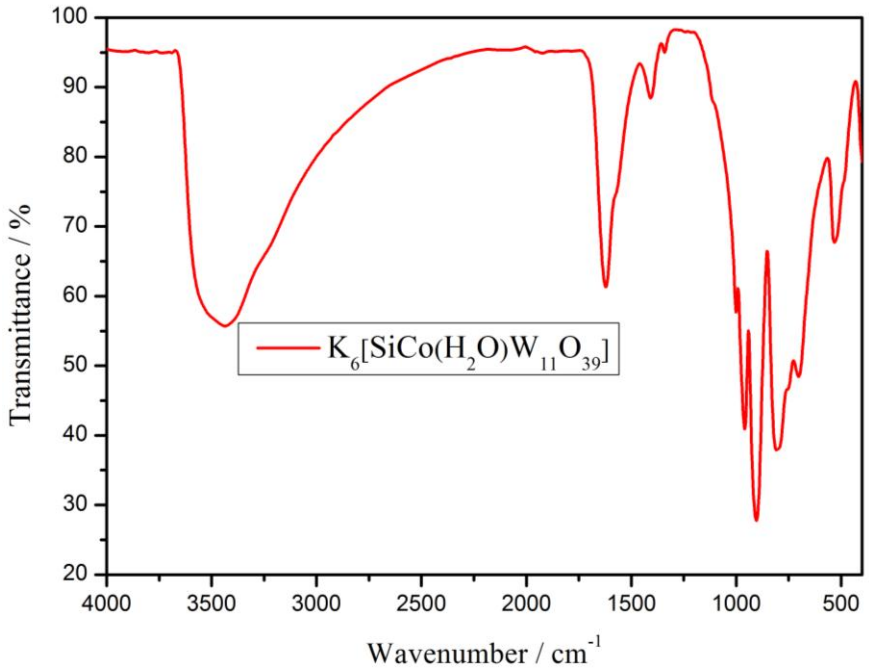

Fig. S5 FT-IR spectrum of **5**.

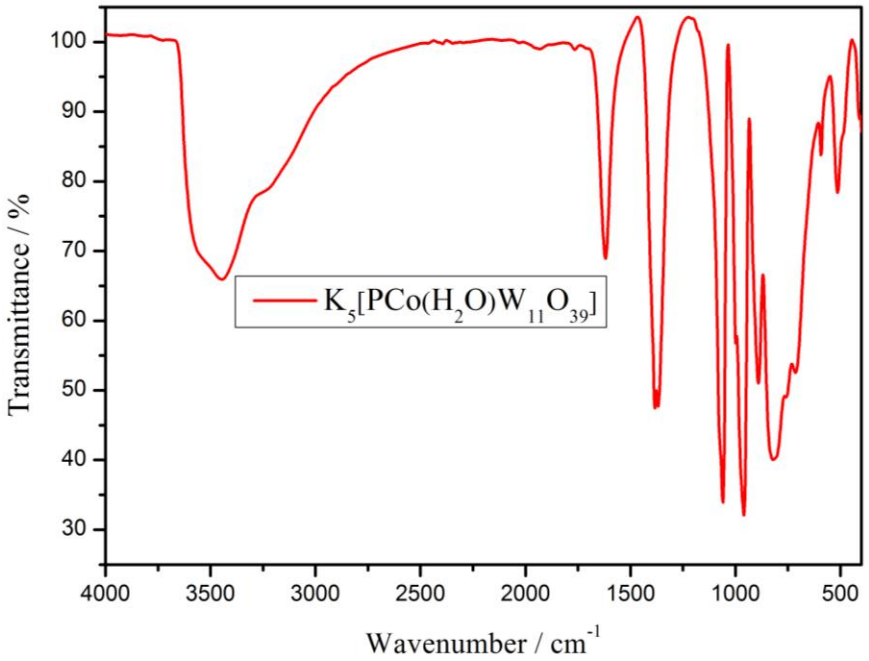

Fig. S6 FT-IR spectrum of **6**.

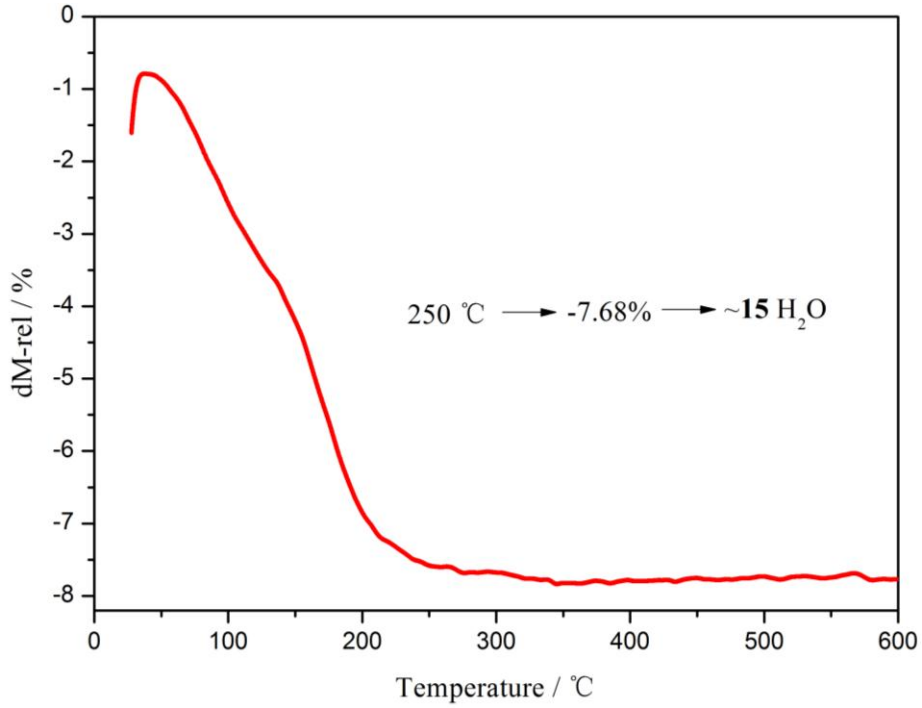

Fig. S7 Thermogravimetric analysis of **1**. The weight loss observed (7.68%) is attributed to waters of hydration and corresponds to 15 water molecules.

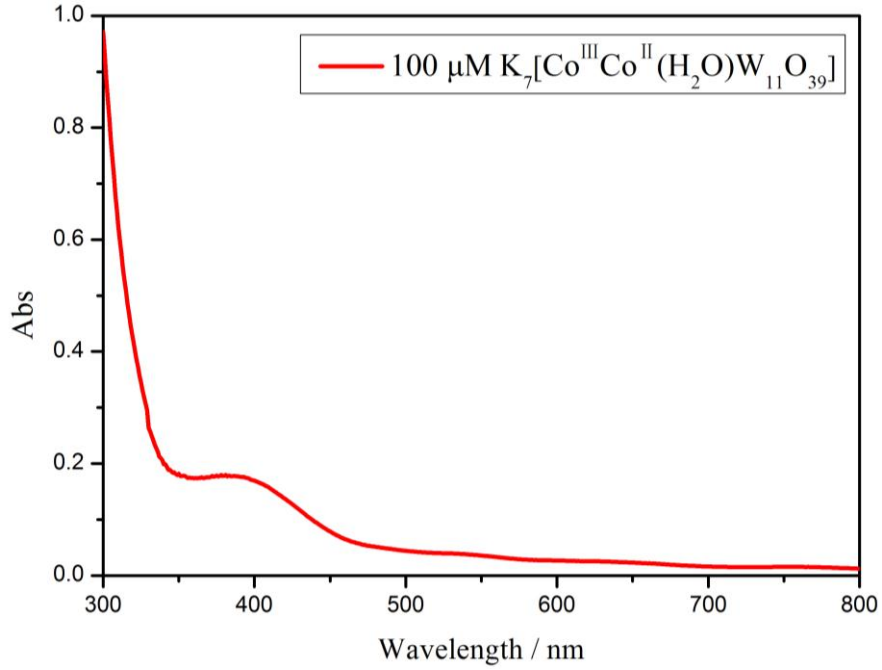

Fig. S8 UV-vis spectrum of 100 μM of **1** in pure water (pH = 7.0).

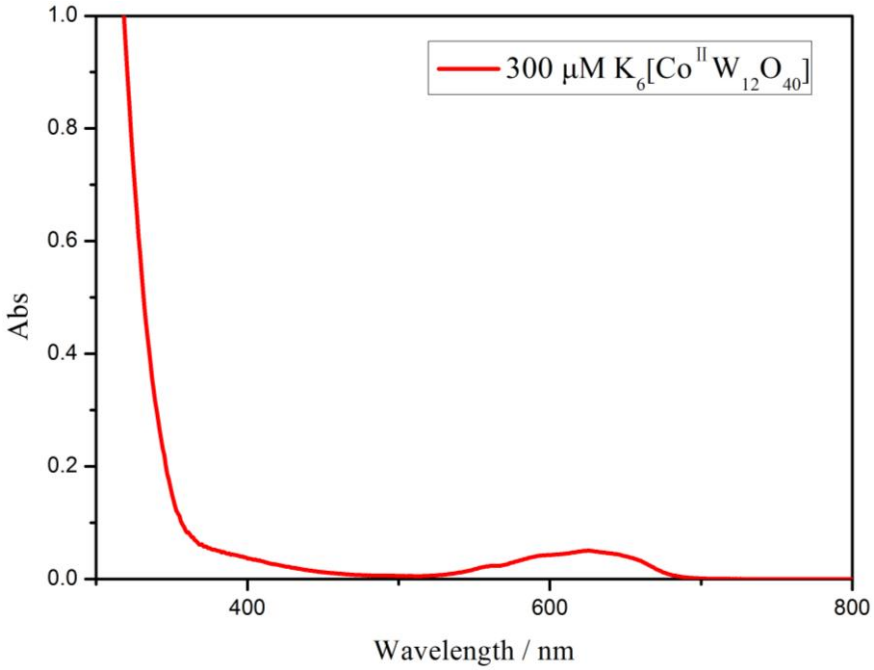

Fig. S9 UV-vis spectrum of 300 μM of **2** in pure water (pH = 7.0).

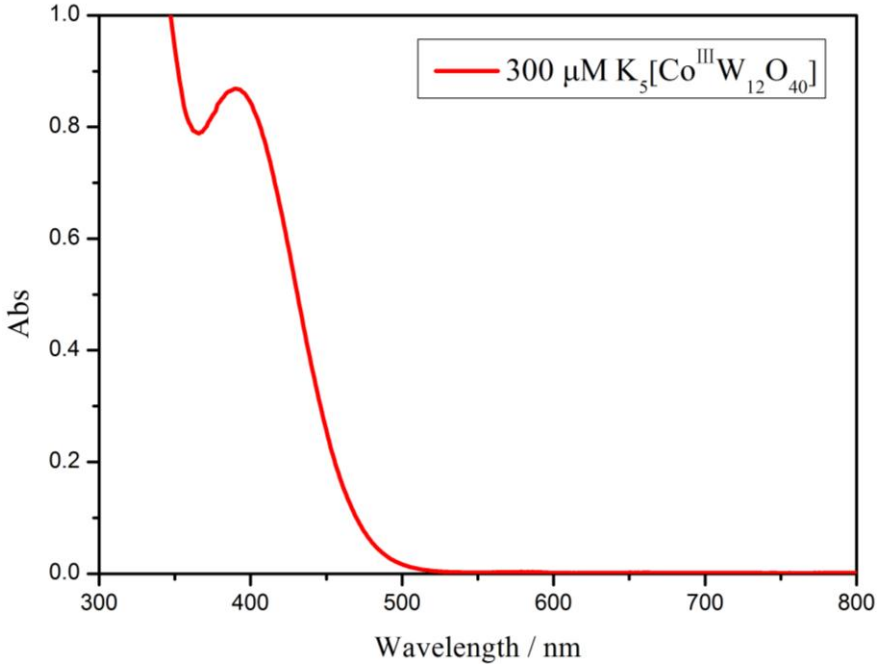

Fig. S10 UV-vis spectrum of 300 μM of **3** in pure water (pH = 7.0).

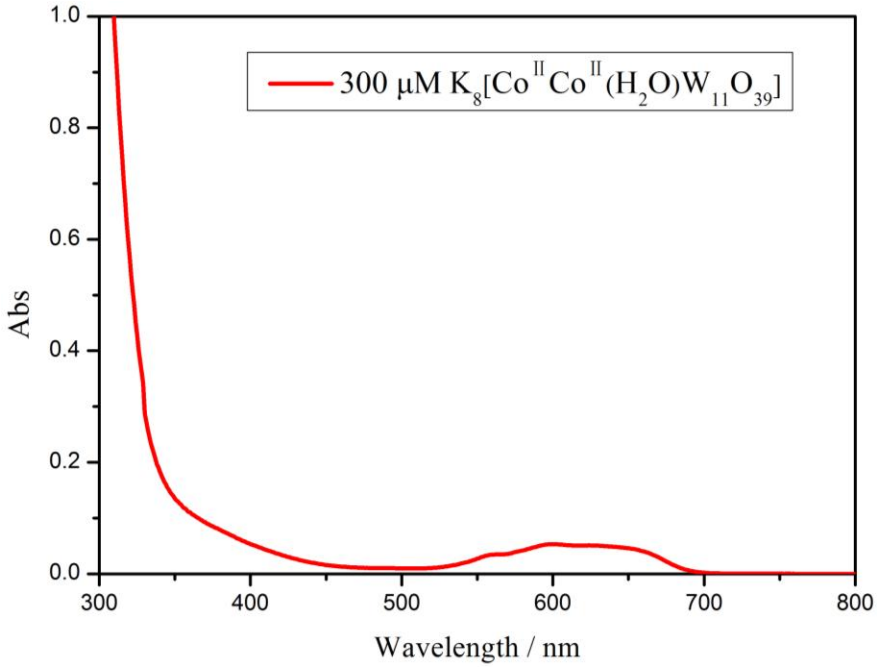

Fig. S11 UV-vis spectrum of 300 μM of **4** in pure water (pH = 7.0).

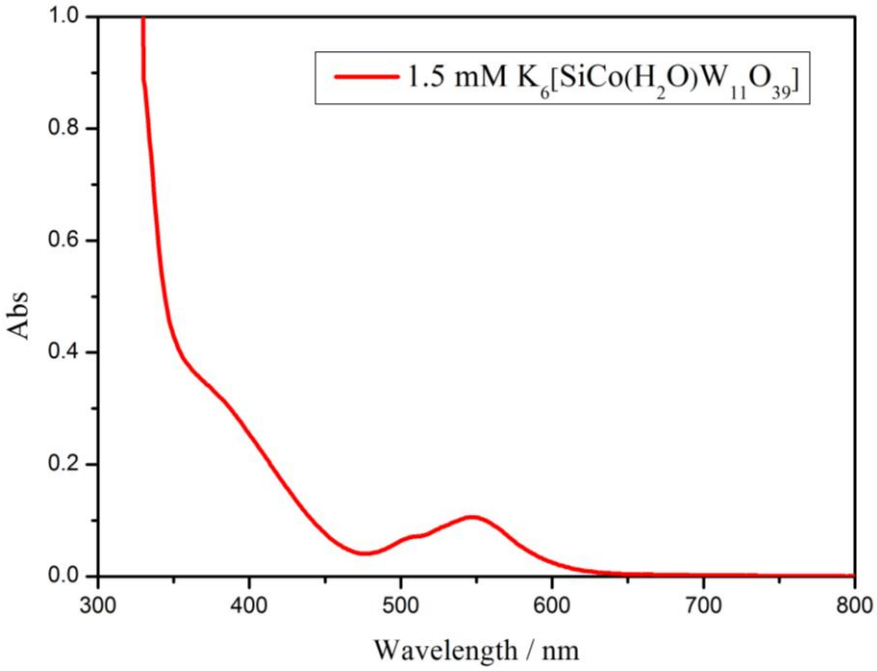

Fig. S12 UV-vis spectrum of 1.5 mM of **5** in pure water (pH = 7.0).

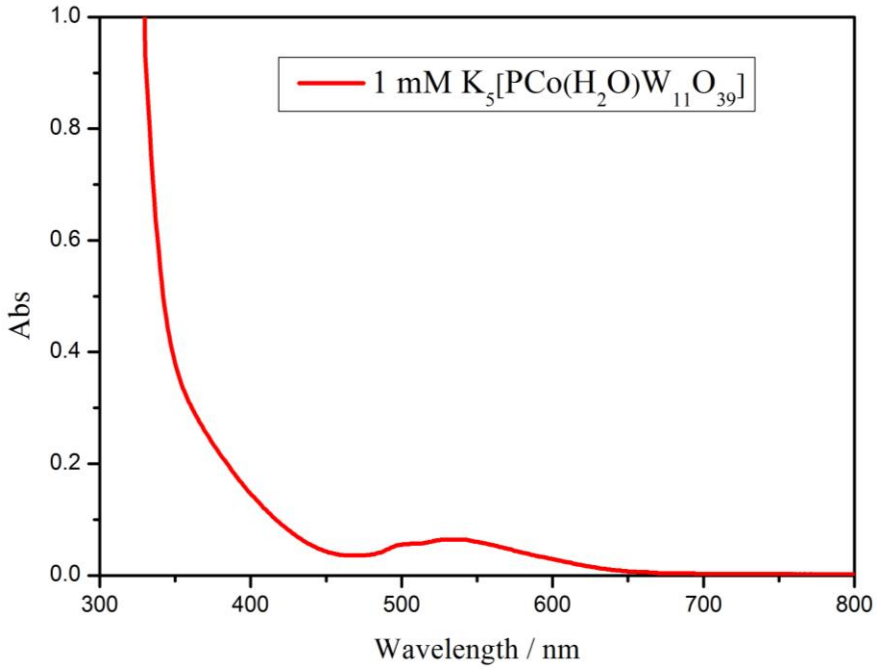

Fig. S13 UV-vis spectrum of 1 mM of **6** in pure water (pH = 7.0).

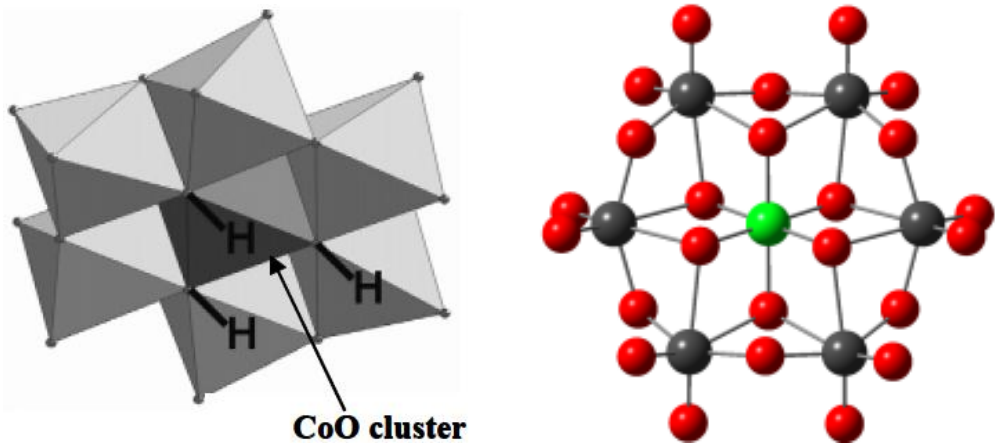

Fig. S14 Structures of Anderson-type $[CoMo_6O_{24}H_6]^{3-}$. In right structure, red ball: oxygen; gray ball: molybdenum; green ball: cobalt. (a) Copyright (2005) American Chemical Society, (b) Copyright (2012) Royal Society of Chemistry.

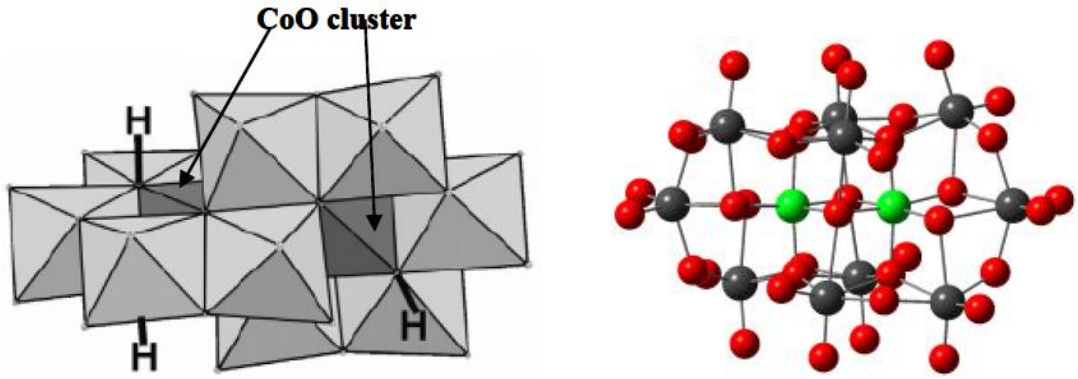

Fig. S15 Structure of Evans-Showell-type $[Co_2Mo_{10}O_{38}H_4]^{6-}$. In right structure, red ball: oxygen; grey ball: molybdenum; green ball: cobalt. (a) Copyright (2005) American Chemical Society, (b) Copyright (2012) Royal Society of Chemistry.

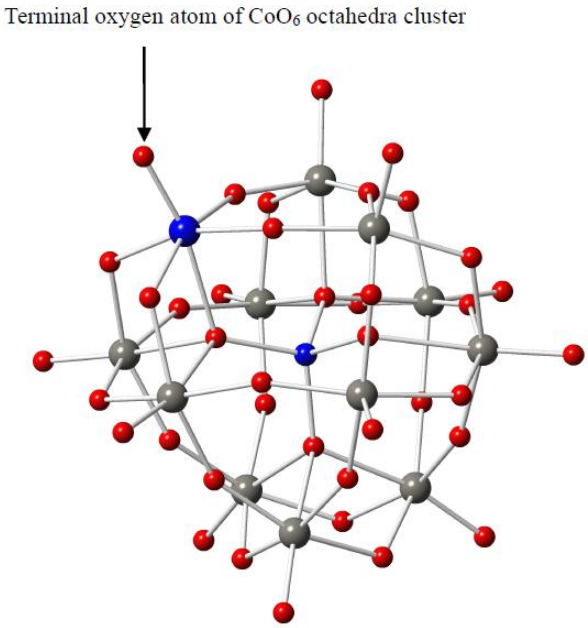

Fig. S16 Structure of Keggin type $[Co^{III}Co^{II}(H_2O)W_{11}O_{39}]^{7-}$, red ball: oxygen; grey ball: tungsten; blue ball: cobalt.

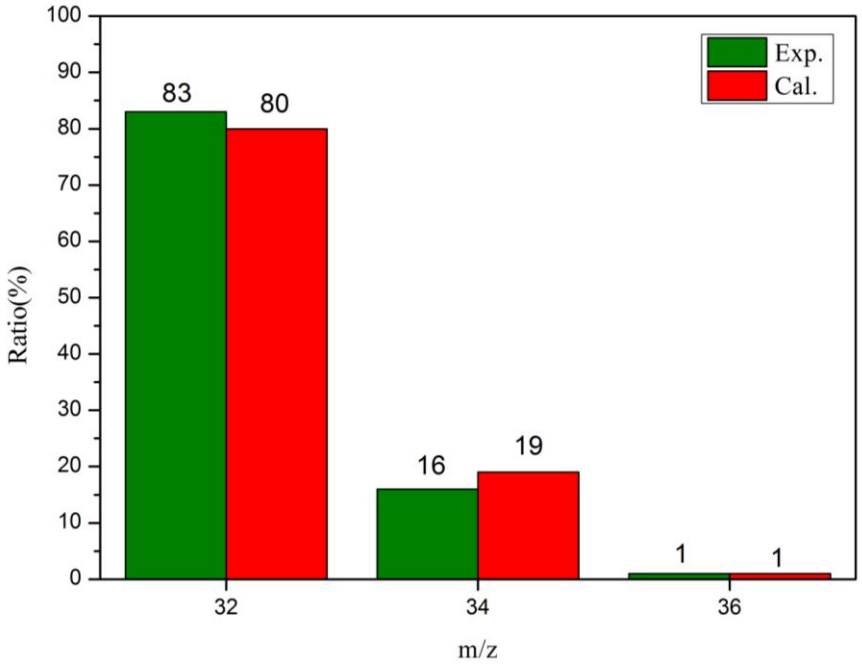

Fig. S17 Observed and theoretical relative abundances of ^{18}O-labeled and unlabeled oxygen evolved during the photocatalytic oxidation of a buffer solution (4.5 mL) prepared with $H_2{}^{18}O$-enriched water (10.8% $H_2{}^{18}O$) containing **1** (15 μM) , $[Ru(bpy)_3]^{2+}$ (1 mM) and $Na_2S_2O_8$ (5 mM) (green, observed mass intensity; red, calculated values assuming that evolved O_2 results exclusively from water).

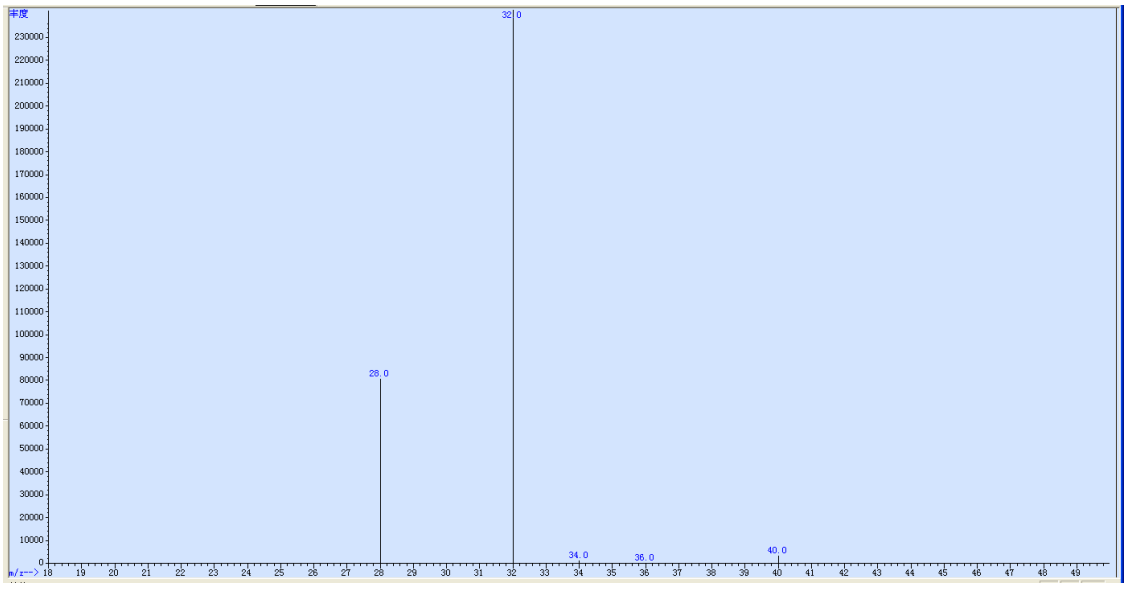

Fig. S18 EI mass spectrum of the gas sample evolved during the irradiation of a buffer solution (4.5 mL) prepared with normal water containing **1** (15 μM) , $[Ru(bpy)_3]^{2+}$ (1 mM) and $Na_2S_2O_8$ (5 mM). The ions with m/z = 28, 32, 34, 36 and 40 were monitored selectively.

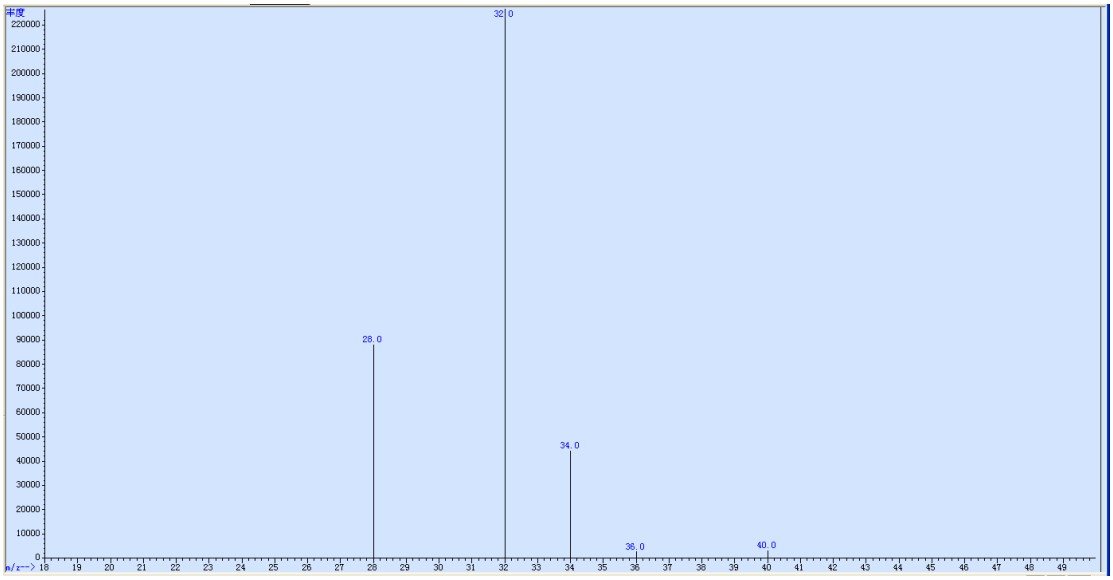

Fig. S19 EI mass spectrum of the gas sample evolved during the photocatalytic oxidation of a buffer solution (4.5 mL) prepared with $H_2{}^{18}O$-enriched water (10.8% $H_2{}^{18}O$) containing **1** (15 μM) , $[Ru(bpy)_3]^{2+}$ (1 mM) and $Na_2S_2O_8$ (5 mM). The ions with m/z = 28, 32, 34, 36 and 40 were monitored selectively.

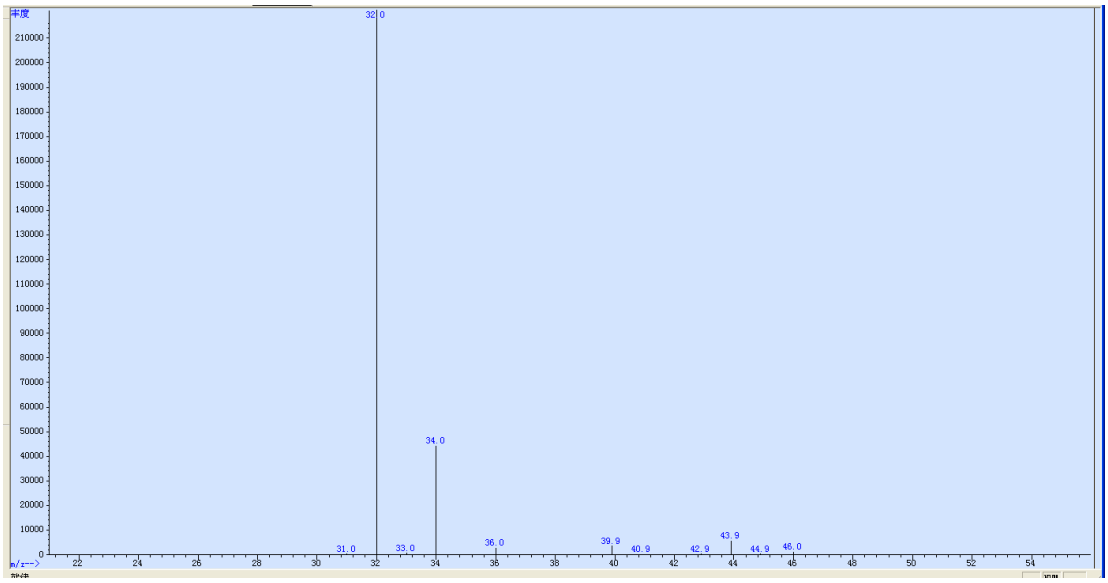

Fig. S20 EI mass spectrum of the gas sample evolved during the photocatalytic oxidation of a buffer solution (4.5 mL) prepared with $H_2{}^{18}O$-enriched water (10.8% $H_2{}^{18}O$) containing **1** (15 μM) , $[Ru(bpy)_3]^{2+}$ (1 mM) and $Na_2S_2O_8$ (5 mM). All ions were monitored.

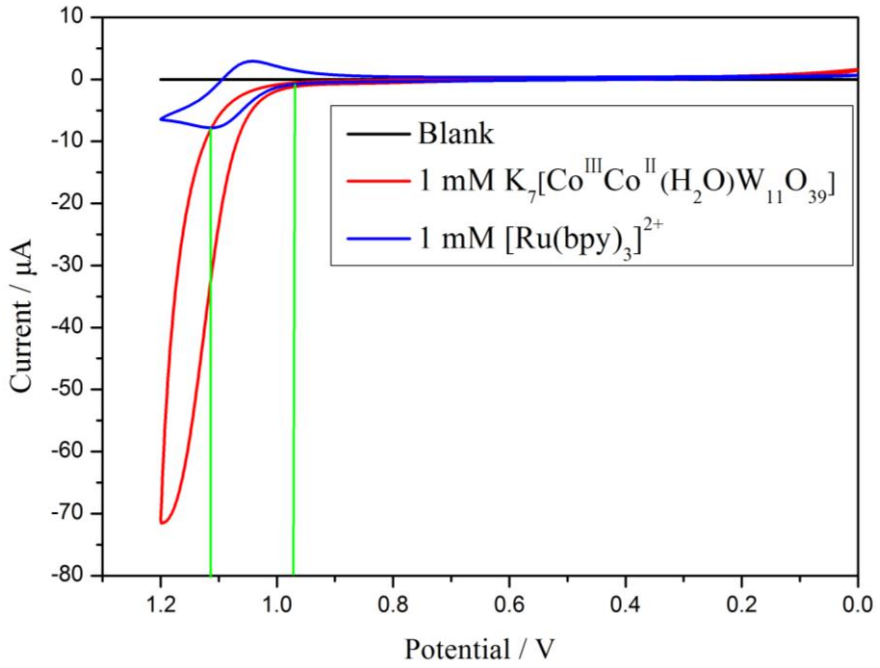

Fig. S21 Cyclic voltammogram (CV) of 80 mM sodium borate buffer solution at pH 9 with 1mM of $[Ru(bpy)_3]Cl_2$ (blue line)and 1 mM of **1**(red line). The black line displays the CV of 80 mM sodium borate buffer solution at pH 9.

			Diam. (nm)	% Intensity	Width (nm)
Z-Average (d.nm):	0.000	Peak 1:	0.000	0.0	0.000
PdI:	0.000	Peak 2:	0.000	0.0	0.000
Intercept:	0.00	Peak 3:	0.000	0.0	0.000
Result quality	Refer to quality report				

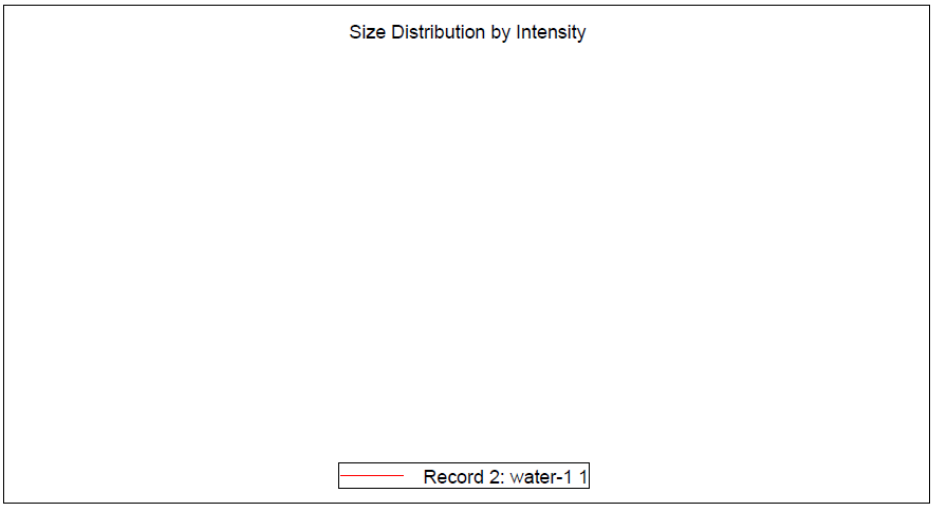

Fig. S22 DLS measurement of a water oxidation reaction solution after 10 min of irradiation shows that no particle exists in photocatalytic water oxidation system.

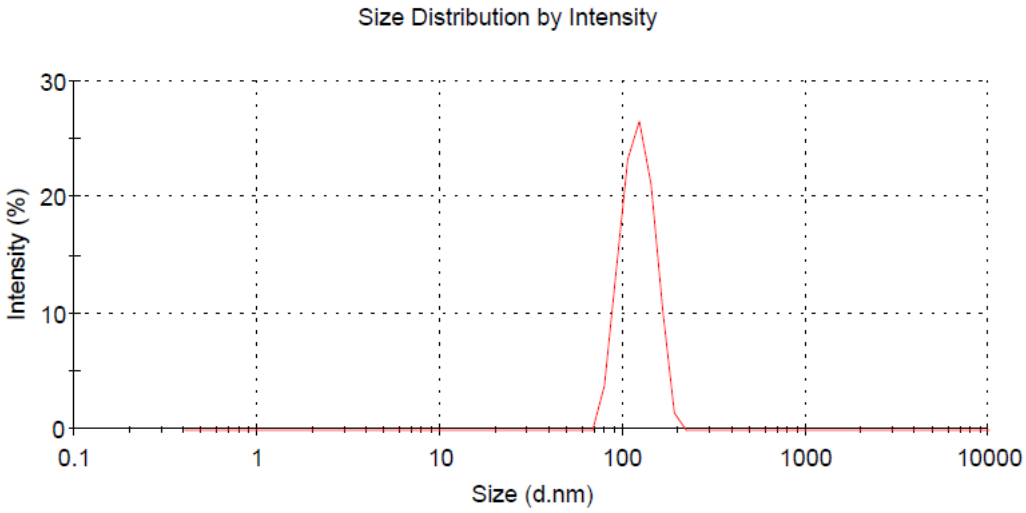

Fig. S23 Particle size distribution measured by DLS in a solution of 99.9% of **1** and 0.1% of $Co(NO_3)_2$ (**1** + $Co(NO_3)_2$ =15 μM), $[Ru(bpy)_3]^{2+}$ (1 mM), $Na_2S_2O_8$ (5 mM) in 80 mM pH 9.0 borate buffer after 10 min of irradiation.

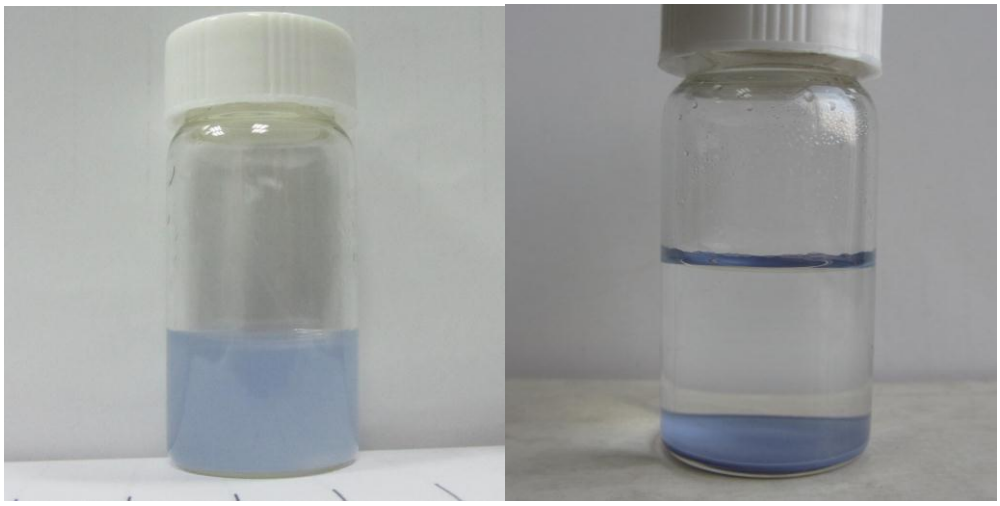

Fig. S24 Compound **4** in borate buffer (80 mM, pH = 9) was aged for 1 h, and purple pink insoluble substance appeared.

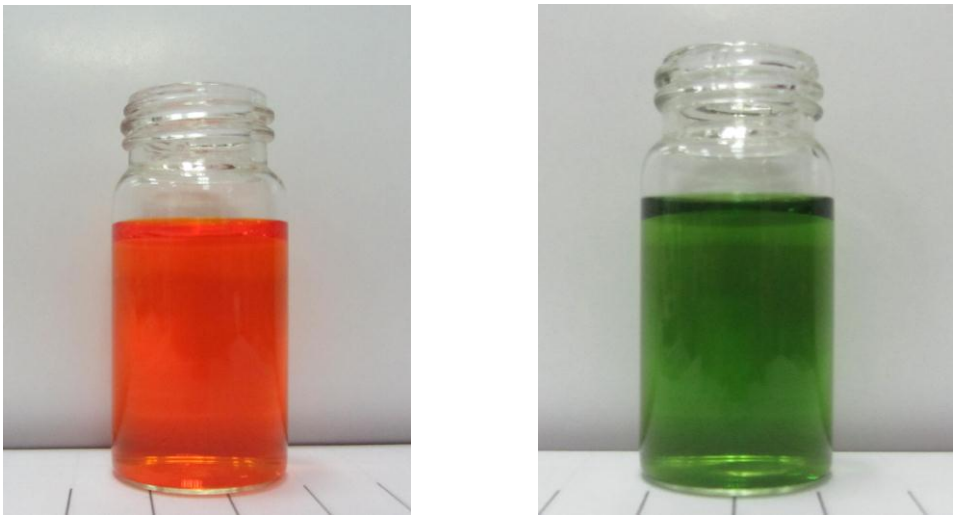

(a) (b)

Fig. S25 (a) Solution containing 1 mM of $[Ru(bpy)_3]^{2+}$ and 5 mM of $Na_2S_2O_8$ in pure water before illumination; (b) Solution containing 1 mM of $[Ru(bpy)_3]^{2+}$ and 5 mM of $Na_2S_2O_8$ in pure water after illumination for 30 s.

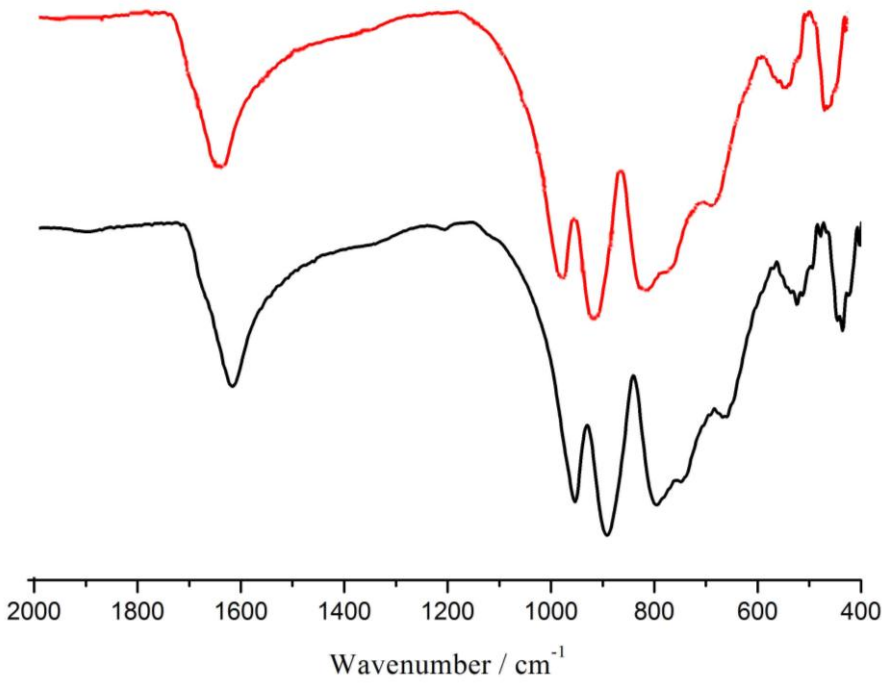

Fig. S26 FT-IR spectra of fresh **1** (black curve) and the recycled catalyst (red curve) obtained from the photocatalytic water oxidation solution using acetone.

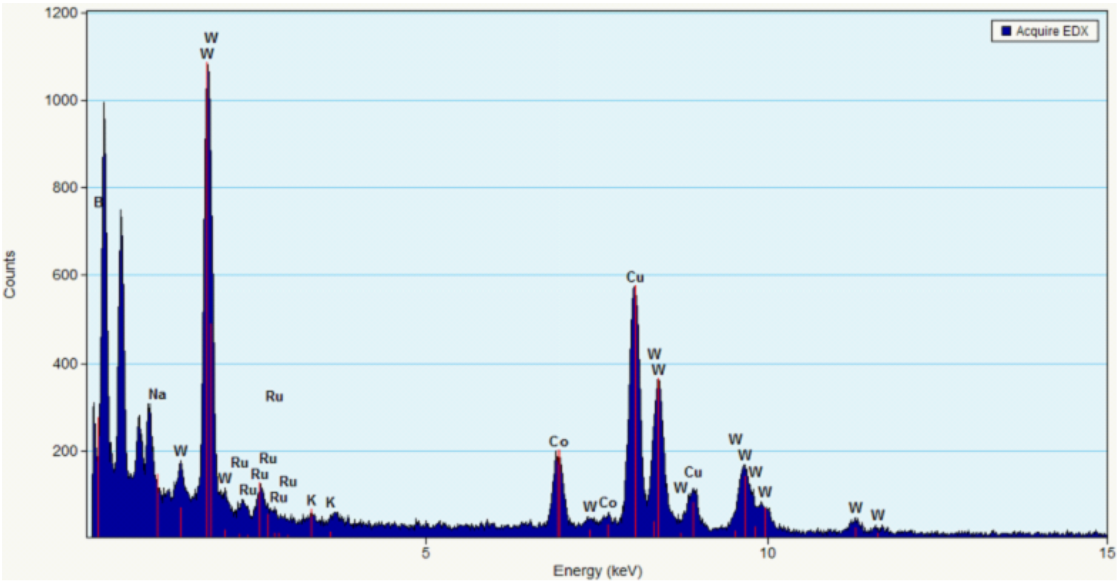

Fig. S27 EDX analysis of precipitate obtained from the photocatalytic water oxidation solution using acetone. W and Co are obviously. The amounts of K, Ru, Na and B are much less than W and Co.

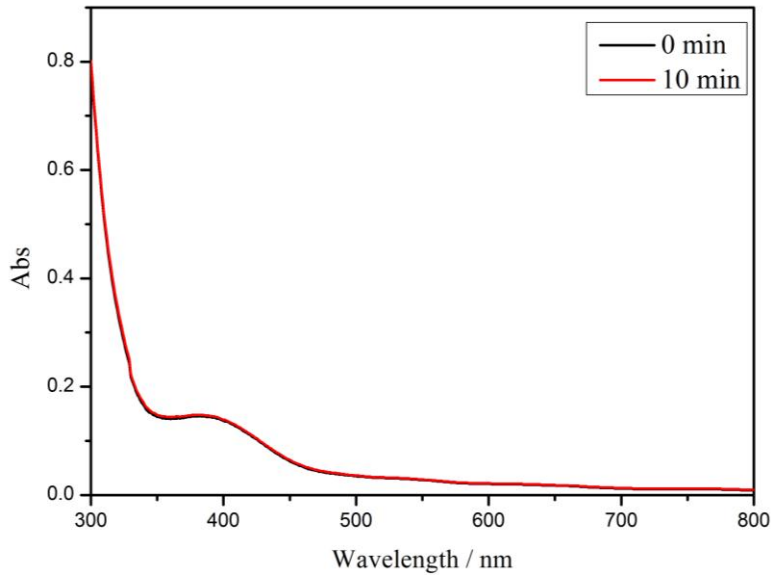

Fig. S28 Time-dependent UV-vis absorption spectra of **1** (100 μM) over 10 min, in borate buffer solution (80 mM, pH 9.0, borate buffer).

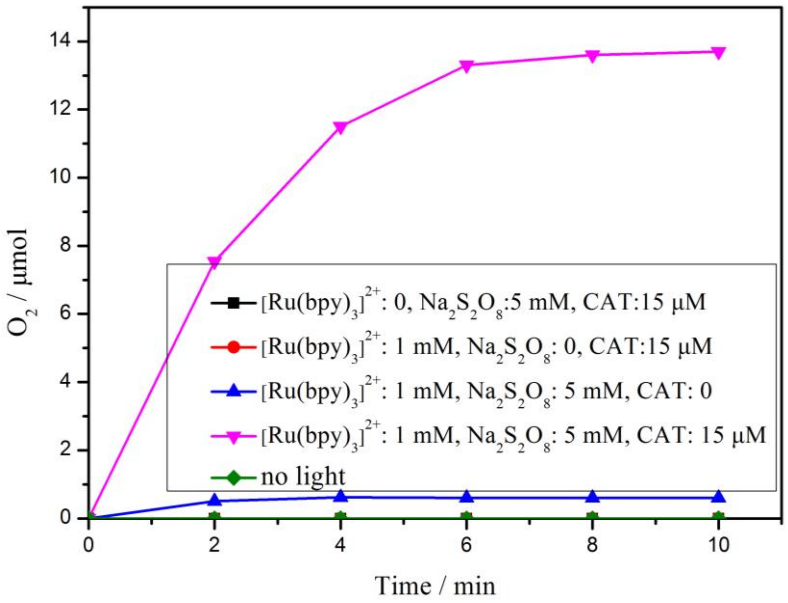

Fig. S29 Kinetics of O_2 formation in the photocatalytic system without **1** (blue), $[Ru(bpy)_3]^{2+}$ (black), $Na_2S_2O_8$ (red) or light (green).

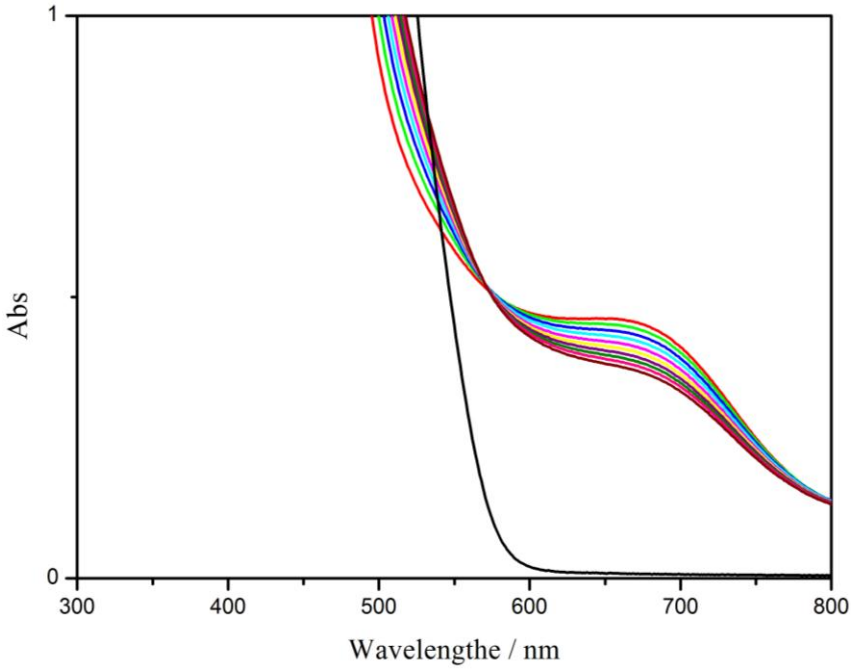

Fig. S30 UV-vis spectral changes during the photocatalytic water oxidation with pH 8.0 buffer. The bottom black line shows the absorption of an aqueous borate buffer solution (pH = 8.0, 80 mM) containing $[Ru(bpy)_3]Cl_2$ (1 mM), $Na_2S_2O_8$ (5 mM)and **1** (15 μM). Other lines show the UV-vis spectral changes of the green reaction solution obtained by irradiatiing the initial reaction solution for 30 s.

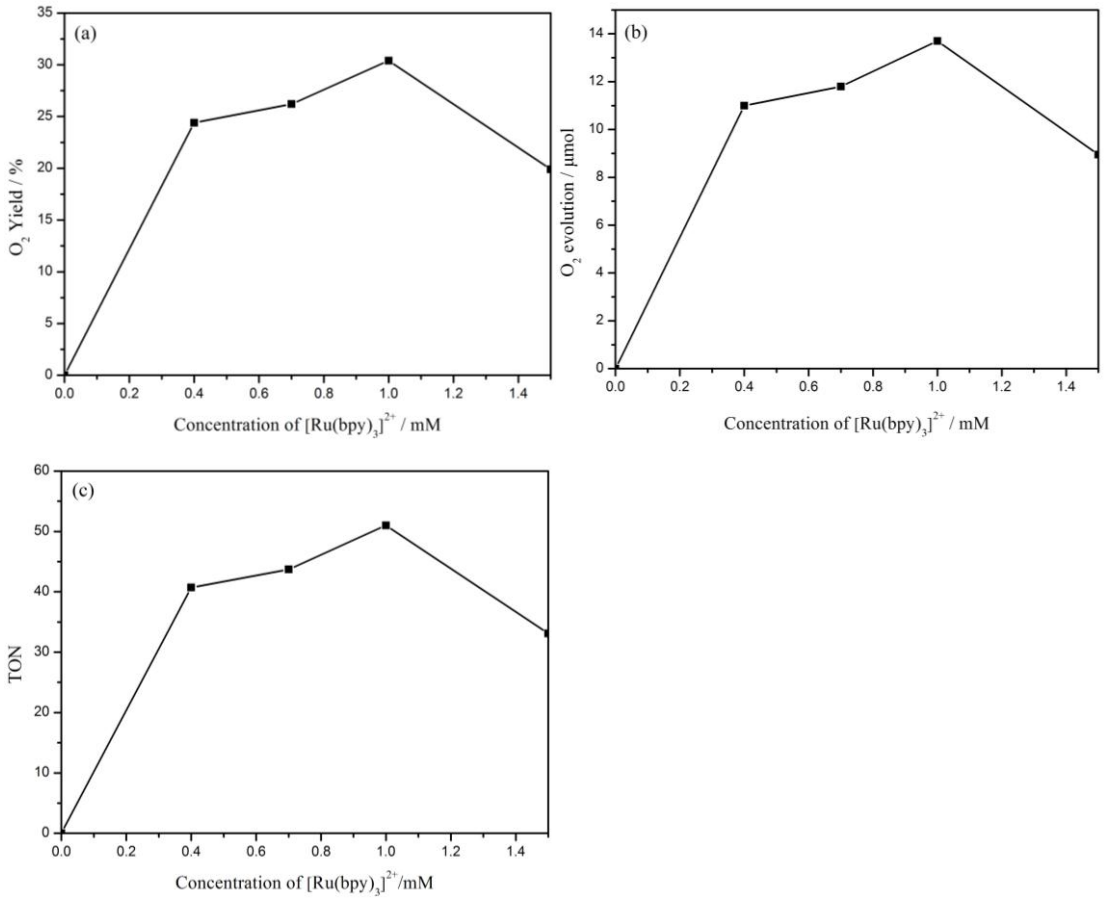

Fig. S31 Dependence of O_2 yield (a), O_2 evolution (b) and TON (c) on concentration of $Na_2S_2O_8$ Conditions: LED lamp (≥ 420 nm), 16 mW; 1.0 mM $[Ru(bpy)_3]^{2+}$, 0–7 mM $Na_2S_2O_8$, 80 mM sodium borate buffer (initial pH 9.0); total reaction volume 18 mL and overall volume is ~25 mL; vigorous agitation using a magnetic stirrer.

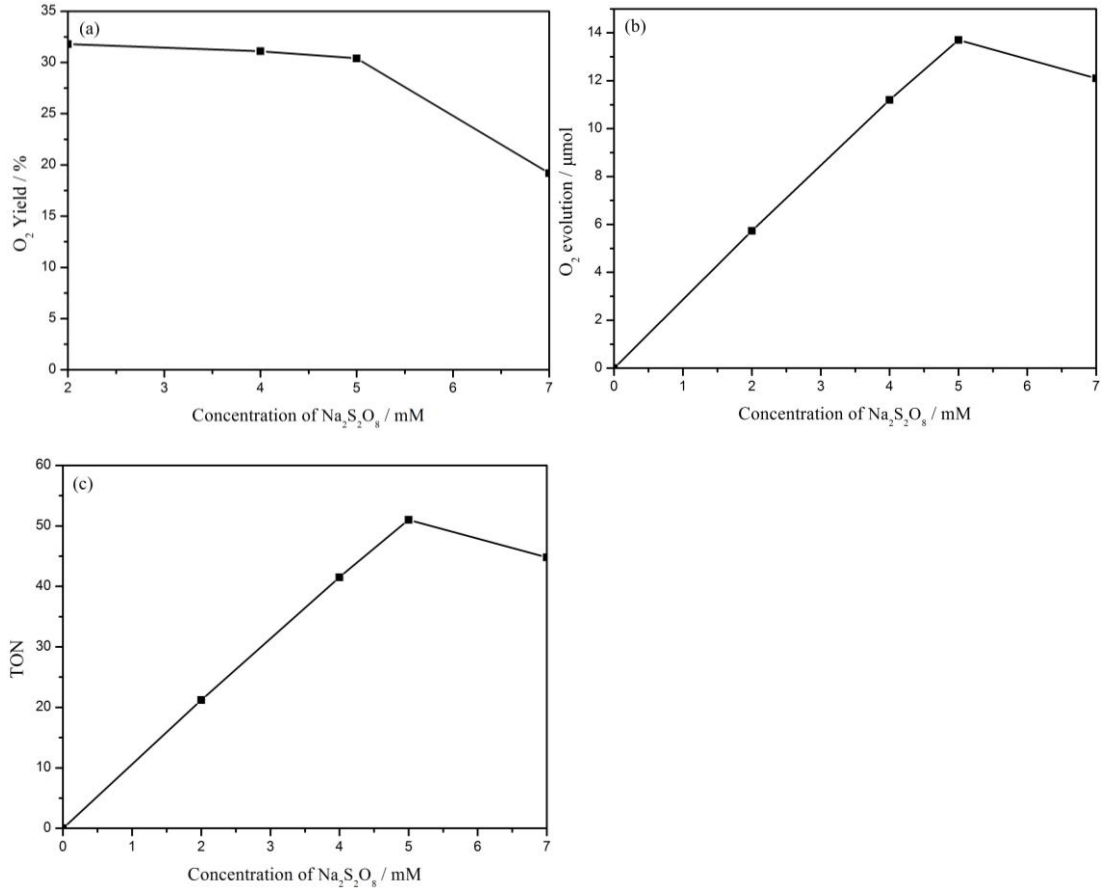

Fig. S32 Dependence of O_2 yield (a), O_2 evolution (b) and TON (c) on concentration of $[Ru(bpy)_3]Cl_2$. Conditions: LED lamp (≥ 420 nm), 16 mW; 0–1.5 mM $[Ru(bpy)_3]^{2+}$, 5 mM $Na_2S_2O_8$, 80 mM sodium borate buffer (initial pH 9.0); total reaction volume 18 mL and overall volume is ~25 mL; vigorous agitation using a magnetic stirrer.

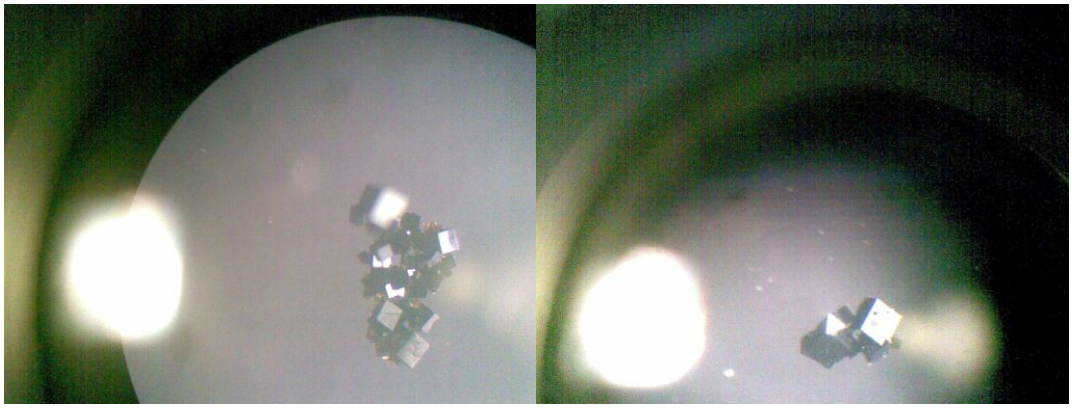

Fig. S33 Images of crystal $K_7[Co^{III}Co^{II}(H_2O)W_{11}O_{39}]$.

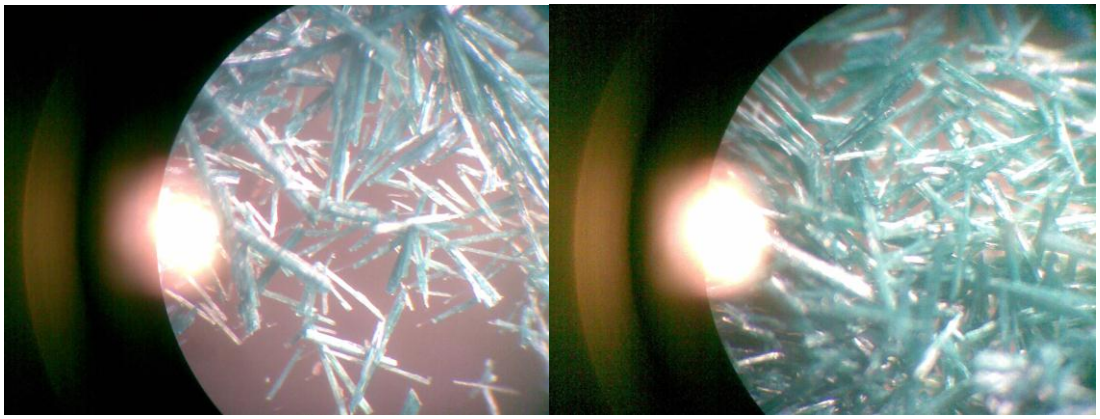

Fig. S34 Images for crystal of $K_6[Co^{II}W_{12}O_{40}]$.

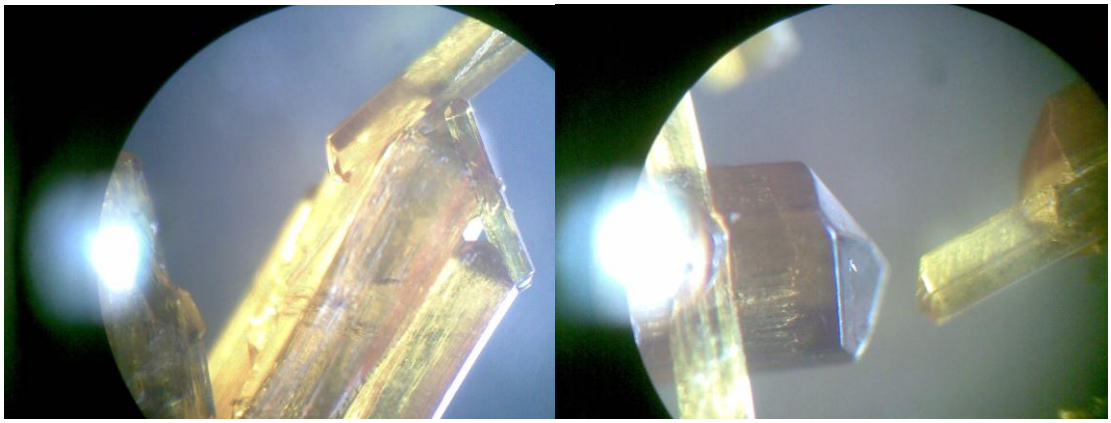

Fig. S35 Images for crystal of $K_5[Co^{III}W_{12}O_{40}]$.

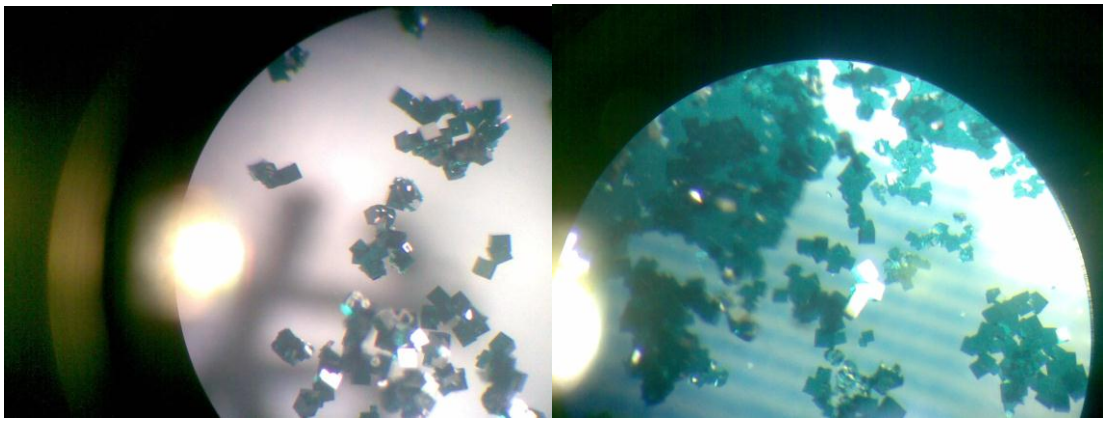

Fig. S36 Images for crystal of $K_8[Co^{II}Co^{II}(H_2O)W_{11}O_{39}]$.

References

1. Z. Huang, Z. Luo, Y. V. Geletii, J. W. Vickers, Q. Yin, D. Wu, Y. Hou, Y. Ding, J. Song, D. G. Musaev, C. L. Hill and T. Lian, *J. Am. Chem. Soc.*, 2011, **133**, 2068-2071.
2. G. Zhu, Y. V. Geletii, P. Kogerler, H. Schilder, J. Song, S. Lense, C. Zhao, K. I. Hardcastle, D. G. Musaev and C. L. Hill, *Dalton Trans.*, 2012, **41**, 2084-2090.
3. S. Tanaka, M. Annaka and K. Sakai, *Chem. Commun.*, 2012, **48**, 1653-1655.
4. P.-E. Car, M. Guttentag, K. K. Baldridge, R. Alberto and G. R. Patzke, *Green Chem.*, 2012, **14**, 1680-1688.
5. C.-F. Leung, S.-M. Ng, C.-C. Ko, W.-L. Man, J. Wu, L. Chen and T.-C. Lau, *Energy Environ. Sci.*, 2012, **5**, 7903-7907.
6. D. Hong, J. Jung, J. Park, Y. Yamada, T. Suenobu, Y.-M. Lee, W. Nam and S. Fukuzumi, *Energy Environ. Sci.*, 2012, **5**, 7606-7616.
7. N. S. McCool, D. M. Robinson, J. E. Sheats and G. C. Dismukes, *J. Am. Chem. Soc.*, 2011, **133**, 11446-11449.
8. G. Chen, L. Chen, S. M. Ng, W. L. Man and T. C. Lau, *Angew. Chem., Int. Ed.*, 2013, **52**, 1789-1791.